Electronic Supplementary Information

Harnessing Bipolar Acceptors for Highly Efficient Exciplex-forming Systems

Yi-Tzu Hung[1,†], Dian Luo[2,3,†], Li-Ming Chen[1], Dun-Cheng Huang[3], Jian-Zhi Wu[3], Yi-Sheng Chen[1], Chih-Hao Chang*[,3] and Ken-Tsung Wong*[,1,4]

[1]Department of Chemistry, National Taiwan University, Taipei 10617, Taiwan

[2]Institute of Lighting and Energy Photonics, National Yang Ming Chiao Tung University, Tainan 71150, Taiwan

[3]Department of Electrical Engineering, Yuan Ze University, Chungli 32003, Taiwan

[4]Institute of Atomic and Molecular Science, Academia Sinica, Taipei 10617, Taiwan

† Equal contributions to this work

Contents		Page

Experimental Section

OLED Fabrication and Characterization

Organic materials and the indium tin oxide (ITO)-coated glass with a sheet resistance of ~15 Ω/square were purchased from Lumtec and Shine Materials Technology. The ITO substrate was washed with deionized water and acetone in sequence, followed by treatment with UV-Ozone for 5 minutes. All organic materials were subjected to temperature gradient sublimation. The organic and metal layers were deposited onto the ITO-coated glass substrate by thermal evaporation, and the device fabrication was completed in a single cycle without breaking the vacuum. Current density-voltage-luminance characterization was measured using a Keithley 238 current source-measure unit and a Keithley 6485 pico-ammeter equipped with a calibrated Si photodiode. The electroluminescent spectra were recorded using an Ocean Optics spectrometer.

Photophysical measurements

All steady-state absorption and emission measurements, transient PL decay measurements, PL quantum yield, and exciplex aging measurements of organic thin films were measured using a Spectrofluorometer (FluoroMax Plus, Horiba Jobin Yvon) with a nitrogen-filled environment. The steady-state absorption and emission, analysis of exciplex PL aging, and PL quantum yield of thin-film characterizations were conducted using an ozone-free xenon arc lamp as the excitation source (λ_{ex}= 305 nm) under ambient conditions. And the PL decay was studied utilizing NanoLED pulsed sources (N-320, Horiba Jobin Yvon) as excitation (λ_{ex}= 320 nm) with the pulse frequency of 50 kHz.

Tables and Figures

Table S1 The OLEDs with pure exciplex emission (exceeding 10% EQE) reported in the literature from 2012 to 2021.

Year	Exciplex system	EL λ_{peak} (nm)	Max. EQE (%)/LE (cd/A)/ PE (lm/W)	$L_{max.}$ (cd/m^2)	Ref.
2012	m-MTDATA:PPT	510	10.0/—/47.0	—	1
2014	mCP:HAP-3MF	550	11.3/—/—	22000	2
2015	TAPC:DPTPCz	503	15.4/45.7/47.9	—	3
2015	TCTA:Tm3PyBPZ	514	13.1/44.2/54.5	—	4
2016	TrisPCz:CN-T2T	530	11.9/37.0/46.5	73800	5
2016	MAC:PO-T2T	514	17.8/52.1/45.5	—	6
2016	TCTA:B4PYMPM	509	11.0/28.9/—	—	7
2016	TAPC:T2T	517	11.6/40.4/42.2	13476	8
2017	DSDTAF:3N-T2T	535	13.2/42.9/45.5	35140	9
	CPTBF:PO-T2T	—	12.5/27.5/33.2	17200	
2018	m-MTDATA:3TPYMB	534	12.9/43.1/—	17100	10
2019	DPSTPA:2CzPN	544	19.0/59.9/62.7	—	11
	DPSTPA:CzDBA	592	14.6/29.6/31.0	—	
2019	mCP:PO-T2T	480	16.0/27.0/26.4	8960	12
	TSBPA:PO-T2T	528	20.0/60.9/71.0	31000	
	TCBPA:POT2T	542	12.8/43.7/45.8	9070	
2019	13AB:POT2T	540	12.4/40.4/43.8	—	13
	13AB:PO-T2T:CDBP	532	15.5/49.9/55.9	—	
	DBT-SADF:PO-T2T	524	16.9/52.4/61.0	—	
	DBT-SADF:PO-	516	20.5/60.0/69.7	—	

	T2T:CDBP				
2019	TAPC:PIM-TRZ	526	21.7/71.2/97.3	35410	14
	TCTA:PIM-TRZ	—	19.1/58.6/69.4	18230	
	Tris-Cz:PIM-TRZ	—	18.6/52.0/71.0	15630	
2020	Tris-PCz:BCz-TRZ	499	11.9/33.6/33.0	—	15
	Tris-PCz:T2T	518	11.5/34.4/33.8	—	
2020	POT2T:DABNA-1	551	10.4/—/—	—	16
2020	TPAFPO:PO-T2T	540	17.0/48.8/63.7	—	17
2020	TAPC:TPCz:	—	16.1/53.2/41.2	—	18
	PCzAC:TPCz	—	17.3/51.3/38.5	—	
	TAPC:TSiCz	—	16.3/52.7/39.8	—	
2020	Tr-Ph:3P-T2T	—	10.3/29.8/37.5	84318	19
	Tr-Ph:3P-T2P	—	10.4/30.8/37.2	37975	
	Tr-Tol:3P-T2P	—	12.8/38.3/46.3	26280	
2020	DEX:PO-T2T	520	11.2/36.0/44.6	—	20
2020	DMAC-DPS:PO-T2T	—	10.8/28.6/—	—	21
2021	DMAC-DPS:PO-T2T	536	10.8/34.9/33.7	—	22
2021	13AB:TRZ-1SO_2	532	11.1/35.7/37.4	—	23
2021	13AB:PO-T2T	544	12.6/43.6/—	—	24
	Pra-2DMAC:PO-T2T	540	15.0/49.2/—	—	
	Prm-2DMAC:PO-T2T	512	10.3/26.9/—	—	
2021	mSiTrz-oCN:mCBP	—	17.6/—/—	—	25
	mSiTrz-mCN:mCBP	—	21.0/—/—	—	
	mSiTrz-pCN:mCBP	—	13.7/—/—	—	
2021	13PXZB:B4PyMPM	560	14.6/43.1/48.3	14080	26

	13PXZB:B3PyMPM	552	10.0/31.7/31.1	9416	
2021	TAPC:**CzT2.1**	543	12.5/39.2/41.4	11406	This work
	TAPC:**CzT2.2**	532	15.0/45.7/50.0	9305	

Table S2 Photophysical and electrochemical data of **CzT2.1** and **CzT2.2**.

	λ_{abs}[a] [nm]	$\lambda_{rt\ PL}$[a] [nm]	$\lambda_{77K\ PL}$[b] [nm]	λ_{Phos}[b] [nm]	HOMO[c] [eV]	LUMO[c] [eV]	E_g[d] [eV]
CzT2.1	284, 330	375, 470	502	489	-5.85	-2.79	3.06
CzT2.2	284, 335, 345	434	418, 448, 479	451, 484, 506	-5.57	-2.77	2.80

[a] Maximum wavelength in toluene solution at room temperature. [b] Maximum wavelength in toluene solution at 77 K. [c] HOMO and LUMO were determined from the electrochemical results in CH_2Cl_2 and DMF solution, respectively. [d] E_g = LUMO – HOMO using electrochemical results.

Table S3 The photophysical characteristics of the exciplex solutions in THF/DI water.

Sample	λ_{PL} [nm]	TRPL [a]					
		A_1	τ_1 [ns]	A_2	τ_2 [ns]	A_3	τ_3 [μs]
A1	543	0.731	227	0.257	502	0.012	2.86
A2	516	0.647	275	0.336	614	0.017	7.97
B1	532	0.760	57	0.098	476	0.142	2.68
B2	511	0.823	37	0.140	180	0.037	2.61

[a] Measured under an ambient atmosphere, and the decay components were fitted with three exponential decay models as $I(t) = A_1 \exp(-t/\tau_1) + A_2 \exp(-t/\tau_2) + A_3 \exp(-t/\tau_3)$.

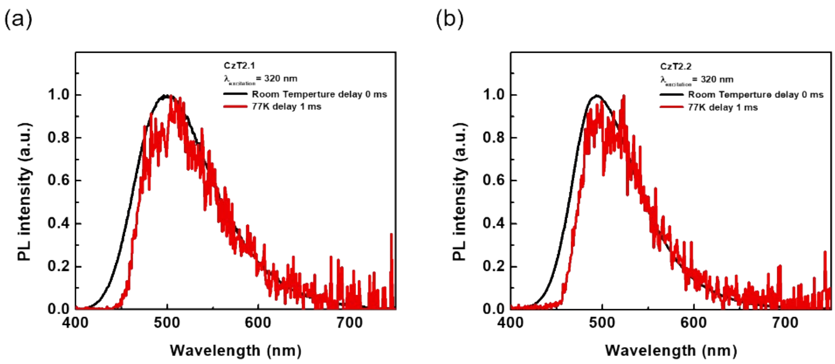

Figure S1 Room temperature and 77K photoluminescence of (a) **CzT2.1** and (b) **CzT2.2** neat films.

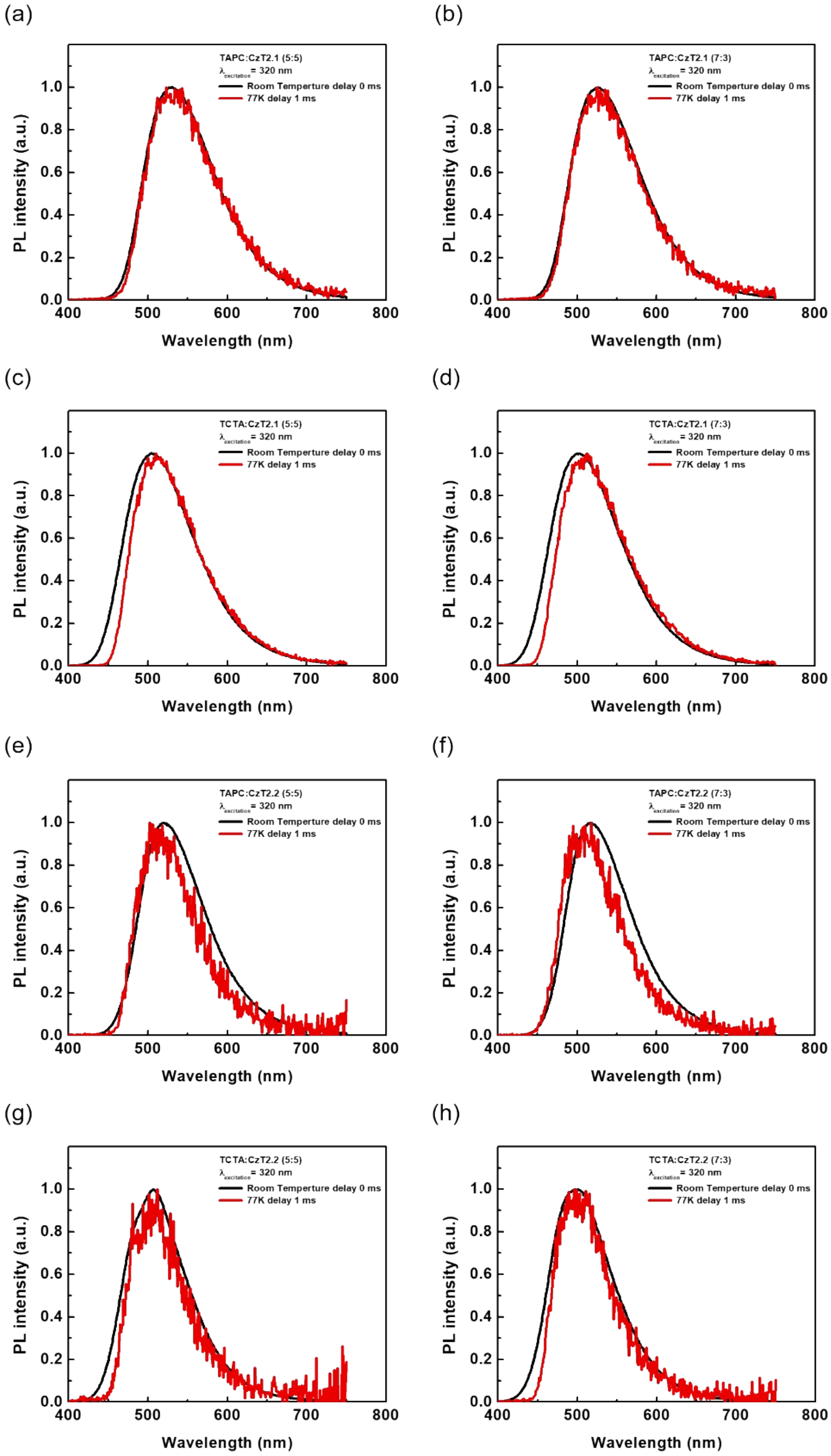

Figure S2 Room temperature and 77K photoluminescence of (a) **A1** (5:5), (b) **A1** (7:3), (c) **A2** (5:5), (d) **A2** (7:3), (e) **B1** (5:5), (f) **B1** (7:3), (g) **B2** (5:5), and (h) **B2** (7:3) blend films.

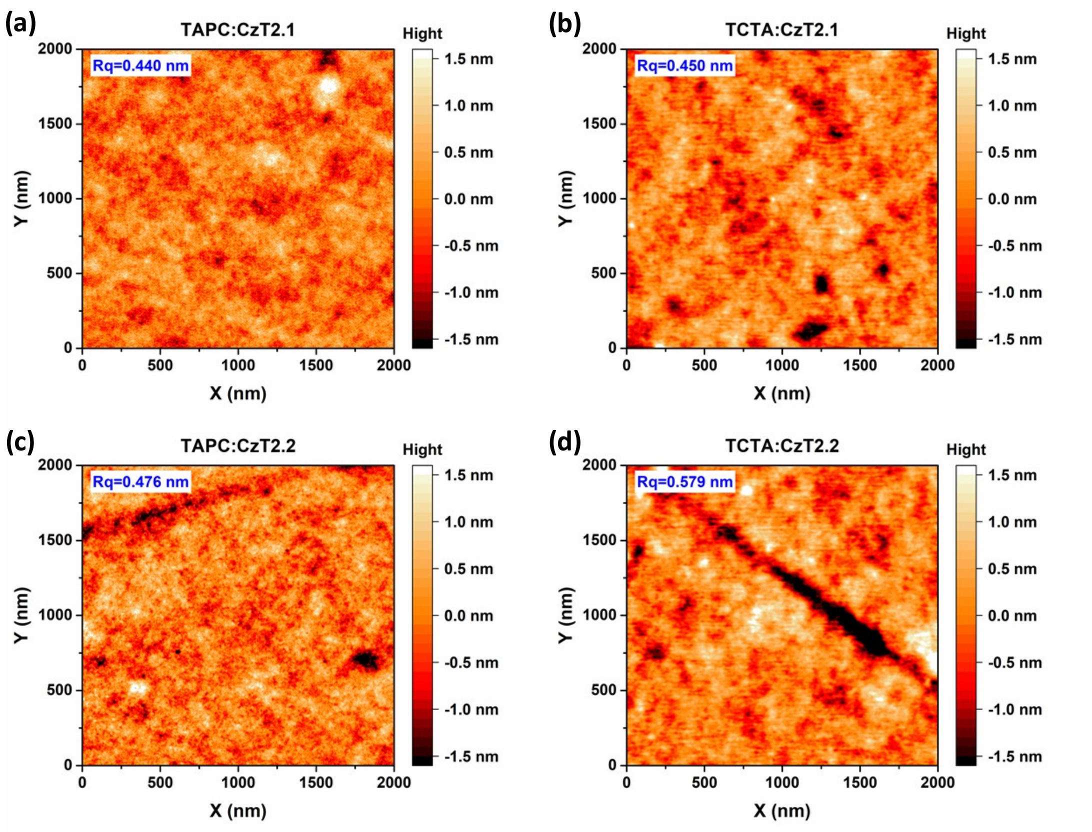

Figure S3 AFM images of four blend samples. (a) **A1** (5:5); (b) **A2** (5:5); (c) **B1** (5:5); (d) **B2** (5:5).

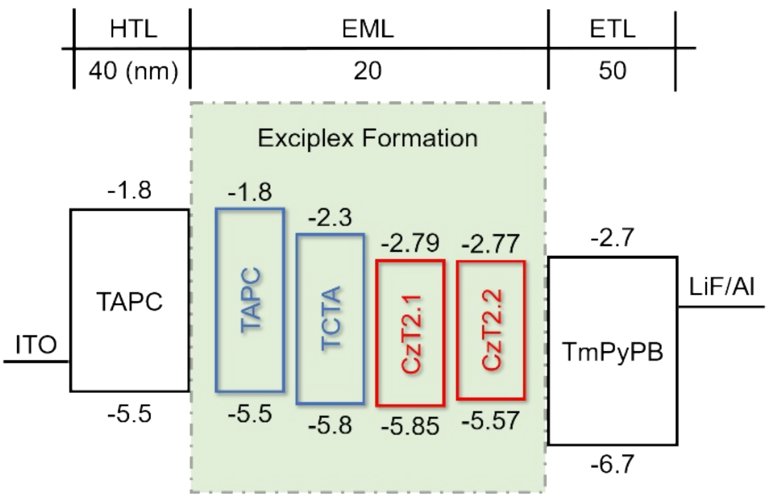

Figure S4 Schematic architecture of the OLED devices.

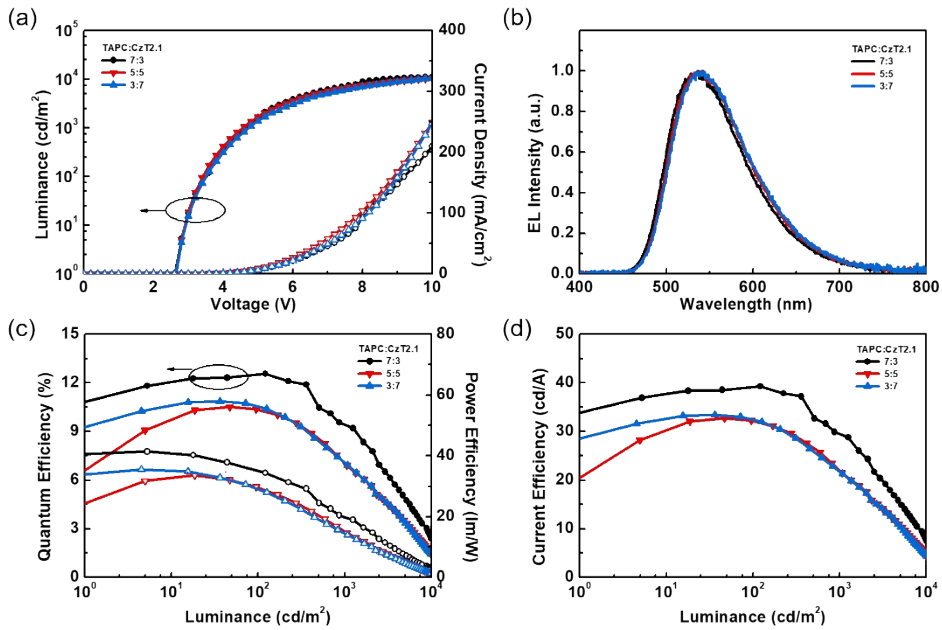

Figure S5 EL characteristics of TAPC:**CzT2.1** devices with different D/A ratios: (a) *J*-*V*-*L* curves, (b) normalized EL spectra, (c) EQE and PE as a function of luminance, and (d) CE-luminance diagram.

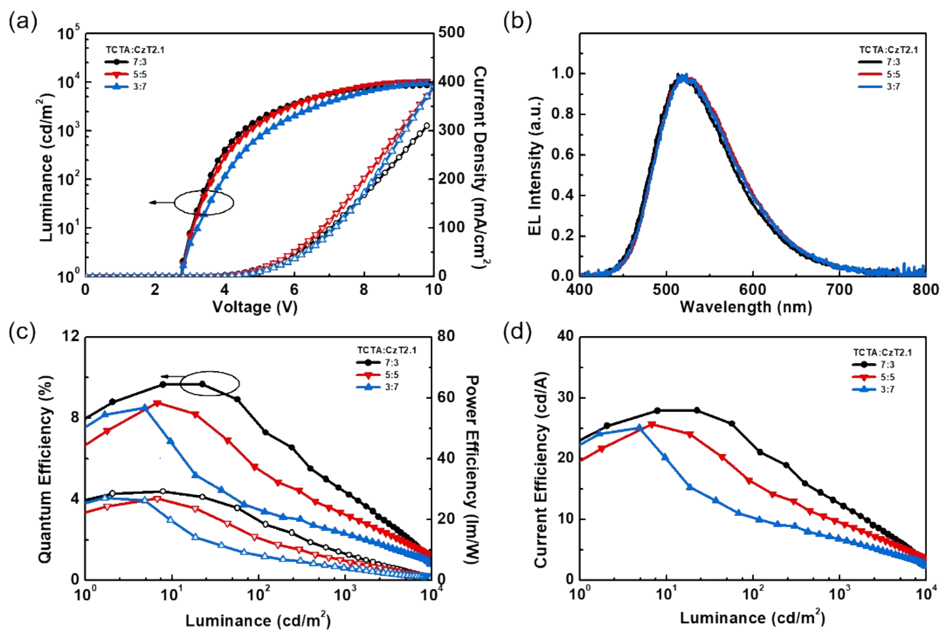

Figure S6 EL characteristics of TCTA:**CzT2.1** devices with different D/A ratios: (a) *J*-*V*-*L* curves, (b) normalized EL spectra, (c) EQE and PE as a function of luminance, and (d) CE-luminance diagram.

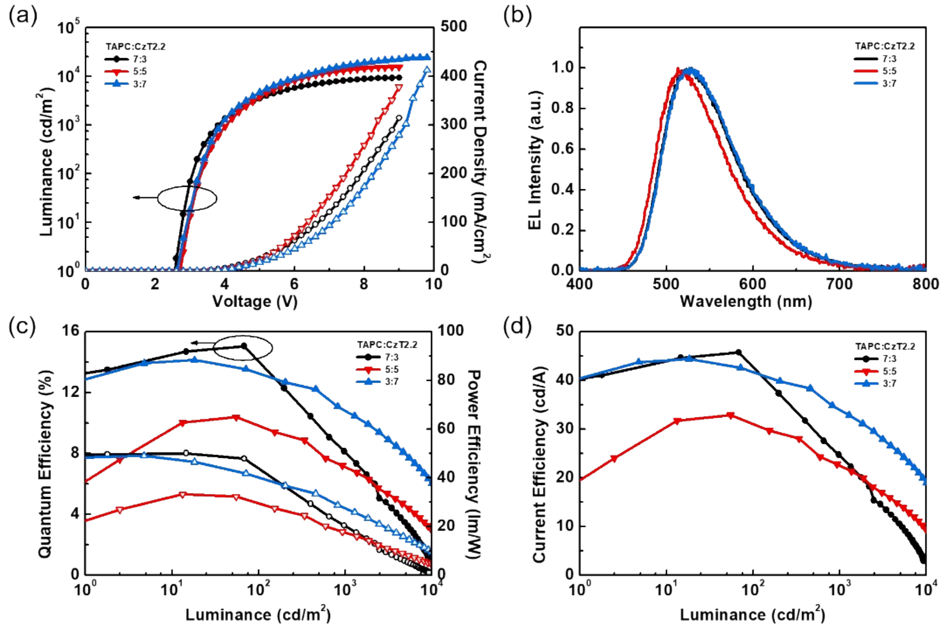

Figure S7 EL characteristics of TAPC:**CzT2.2** devices with different D/A ratios: (a) *J-V-L* curves, (b) normalized EL spectra, (c) EQE and PE as a function of luminance, and (d) CE-luminance diagram.

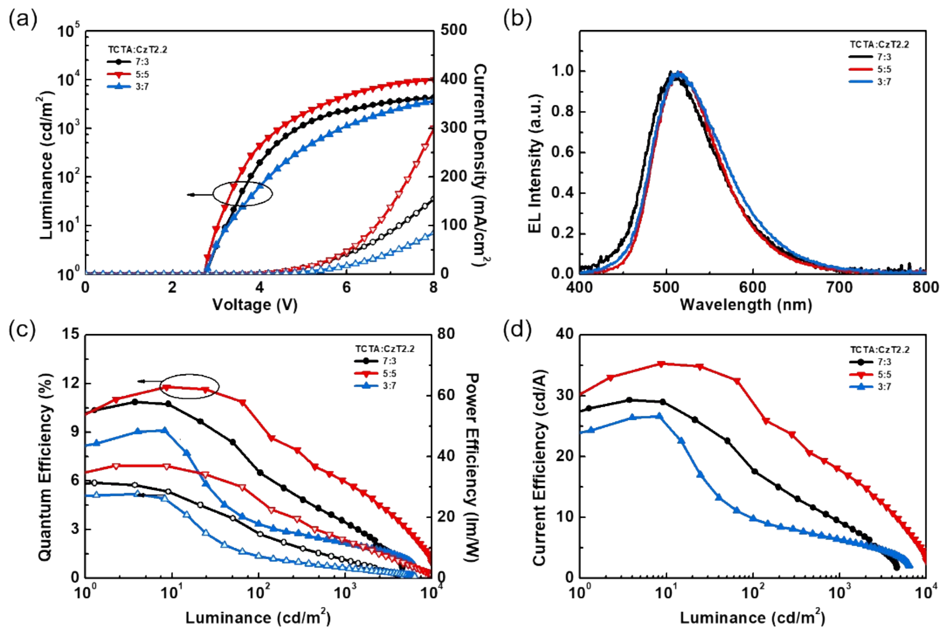

Figure S8 EL characteristics of TCTA-hosted devices with different **CzT2.2**-doping ratios: (a) *J-V-L* curves, (b) normalized EL spectra, (c) EQE and PE as a function of luminance, and (d) CE-luminance diagram.

References

1 K. Goushi and C. Adachi, *Appl. Phys. Lett.*, 2012, **101**, 023306.

2 J. Li, H. Nomura, H. Miyazaki and C. Adachi, *Chem. Commun.,* 2014, **50**, 6174-6176.

3 X.-K. Liu, Z. Chen, C.-J. Zheng, C.-L. Liu, C.-S. Lee, F. Li, X.-M. Ou and X.-H. Zhang, *Adv. Mater.*, 2015, **27**, 2378-2383.

4 L. Zhang, C. Cai, K. F. Li, H. L. Tam, K. L. Chan and K. W. Cheah, *ACS Appl. Mater. Interfaces*, 2015, **7**, 24983-24986.

5 W.-Y. Hung, P.-Y. Chiang, S.-W. Lin, W.-C. Tang, Y.-T. Chen, S.-H. Liu, P.-T. Chou, Y.-T. Hung and K.-T. Wong, *ACS Appl. Mater. Interfaces*, 2016, **8**, 4811-4818.

6 W. Liu, J.-X. Chen, C.-J. Zheng, K. Wang, D.-Y. Chen, F. Li, Y.-P. Dong, C.-S. Lee, X.-M. Ou and X.-H. Zhang, *Adv. Funct. Mater.*, 2016, **26**, 2002-2008.

7 K.-H. Kim, S.-J. Yoo and J.-J. Kim, *Chem. Mater.*, 2016, **28**, 1936-1941.

8 T. Lin, T. Zhang, Q. Song, F. Jin, Z. Liu, Z. Su, Y. Luo, B. Chu, C. S. Lee and W. Li, *Org. Electron.*, 2016, **38**, 69-73.

9 W.-Y. Hung, T.-C. Wang, P.-Y. Chiang, B.-J. Peng and K.-T. Wong, *ACS Appl. Mater. Interfaces*, 2017, **9**, 7355-7361.

10 Q. Huang, S. Zhao, P. Wang, Z. Qin, Z. Xu, D. Song, B. Qiao and X. Xu, *J. Lumin.*, 2018, **201**, 38-43.

11 T.-L. Wu, S.-Y. Liao, P.-Y. Huang, Z.-S. Hong, M.-P. Huang, C.-C. Lin, M.-J. Cheng and C.-H. Cheng, *ACS Appl. Mater. Interfaces*, 2019, **11**, 19294-19300.

12 M. Chapran, P. Pander, M. Vasylieva, G. Wiosna-Salyga, J. Ulanski, F. B. Dias and P. Data, *ACS Appl. Mater. Interfaces*, 2019, **11**, 13460-13471.

13 M. Zhang, W. Liu, C.-J. Zheng, K. Wang, Y.-Z. Shi, X. Li, H. Lin, S.-L. Tao and X.-H. Zhang, *Adv. Sci.*, 2019, **6**, 1801938.

14 B. Liang, J. Wang, Z. Cheng, J. Wei and Y. Wang, *J. Phys. Chem. Lett.*, 2019, **10**, 2811-2816.

15 T. B. Nguyen, H. Nakanotani, T. Hatakeyama and C. Adachi, *Adv. Mater.*, 2020, **32**, e1906614.

16 K. H. Lee and J. Y. Lee, *Adv. Opt. Mater.*, 2020, **8**, 2000328.

17 J. Zhao, J. Ye, X. Du, C. Zheng, Z. He, H. Yang, M. Zhang, H. Lin and S. Tao, *Asian J. Org. Chem.*, 2020, **15**, 4093-4097.

18 H. J. Jang and J. Y. Lee, *J. Phys. Chem. C*, 2020, **124**, 15057-15065.

19 Y.-C. Hu, Z.-L. Lin, T.-C. Huang, J.-W. Lee, W.-C. Wei, T.-Y. Ko, C.-Y. Lo, D.-G. Chen, P.-T. Chou, W.-Y. Hung and K.-T. Wong, *Mater. Chem. Front.*, 2020, **4**, 2029-2039.

20 Q.-S. Tian, X.-D. Zhu and L.-S. Liao, *Mater. Chem. Front.*, 2020, **4**, 1648-1655.

21 S. K. Jeon and J. Y. Lee, *Org. Electron.*, 2020, **76**, 105477.

22 Q. Ren, Y. Zhao, C. Liu, H. Zhan, Y. Cheng and W. Li, *Opt. Mater.*, 2021, **112**, 110779.

23 J. Guo, C.-J. Zheng, K. Ke, M. Zhang, H.-Y. Yang, J.-W. Zhao, Z.-Y. He, H. Lin, S.-L. Tao and X.-H. Zhang, *J. Mater. Chem. C*, 2021, **9**, 939-946.

24 N. Zhang, C. Zheng, Z. Chen, J. Zhao, M. Zhang, H. Yang, Z. He, X. Du and S. Tao, *J. Mater. Chem. C*, 2021, **9**, 600-608.

25 J. H. Yun, K. H. Lee, W. J. Chung, J. Y. Lee, Y. Lee and J. J. Lyu, *Chem. Eng. J.*, 2021, **417**, 128086.

26 M. Zhang, C.-J. Zheng, K. Wang, Y.-Z. Shi, D.-Q. Wang, X. Li, H. Lin, S.-L. Tao and X.-H. Zhang, *Adv. Funct. Mater.*, 2021, **31**, 2100064.